Oscillations and Island Evolution in Radiating Diffusion Flames

Milan Miklavčič*, Amy B. Moore
Department of Mathematics, Michigan State University, East Lansing, MI 48824, USA

Indrek S. Wichman†
Department of Mechanical Engineering, Michigan State University, East Lansing, MI 48824, USA

July 29, 2005

Abstract

We show how an island (isola) evolves out of the usual S-curve of steady states of diffusion flames when radiation losses are accounted for and how it eventually disappears when radiation increases further. At small activation temperatures there are never any islands. We show that stable oscillations evolve first out of perturbations of steady states on the S-curve at large Damköhler numbers. Only if, the activation temperature is large enough they do appear also on the islands. The region of the stable oscillations grows larger as activation temperature decreases.

Keywords: Diffusion flames, Hopf bifurcation, stable oscillations, stable limit cycle

1 Introduction

The theoretical and numerical examination of the response of a pure diffusion flame (in which the physics include only diffusion, chemical reaction, and possibly convection: volumetric heat losses by radiation or other means are not considered) to small perturbations using analytical and numerical techniques has produced a clear picture of the expected flame behavior. In particular, Vance et al. [14], characterizes it through extensive numerical study of the eigenvalues of the linearized equations. Kukuck and Matalon [8] later used the method of matched asymptotic expansions. Earlier studies by Kim and coworkers used high activation energy asymptotic techniques to study the stability problem, see [5, 6, 7]. Cheatham and Matalon [2] provided a detailed and lengthy discussion and asymptotic formulation of the stability of diffusion flames in the large-activation energy limit. One of the outcomes of these stability analyses is the predictions for flame oscillations. In particular, Kim and coworkers [5, 7] predicted a pulsating instability when the Lewis number is slightly greater than unity. Sohn et al [11] observed, by direct numerical simulation, decaying oscillations and oscillations leading to flame extinction. A stability analysis by

* *e-mail:* milan@math.msu.edu
† Supported in part by the NASA - Glenn Microgravity Combustion Program, NCC3-662

Vance et al. [14] gave a description of conditions under which oscillations can occur. This analysis did not address long term behaviors of the oscillations.

In the later 1990s studies also were made of heat-losing diffusion flames. Perhaps the first of these articles is the work of Cheatham and Matalon [1] in which the volumetric heat loss term in the energy equation is linearized as $h(T - T_0)$. Kukuck and Matalon [8] used the same model and looked at the modifications of the S-curve of steady flames only near the upper turn. Sohn et al. ([12]) used the nonlinear optically thin radiation approximation $RD(T^4 - T_0^4)$ and obtained an island of steady state flames instead of the S-curve. On the back of the island (i.e for large Damkohler number) they found a small region of unstable steady flames which, when perturbed, evolved into stable oscillations. Nothing like that was ever reported before. The recent numerical study of Christiansen et al. [3] still used the optically thin volumetric radiant heat-loss approximation. However, it incorporated variable properties and full species multicomponent diffusion, as well as detailed multistep reaction chemistry. They were not able to find stable oscillations during their many numerical simulations. They explain that this is due either to the different geometry (i.e. spherical not planar [14, 11, 12]) or to the fact that the stable oscillations appeared only in "an extremely narrow regime." Here we show that the region of stable oscillations is actually very large for flames with small activation energy, in which case the stable oscillations appear on the transformed S-curve and not on the island. We also show how the islands develop from the S-curve and how they eventually disappear as the radiation losses increase.

2 Mathematical model

We assume that fuel issues from the large reservoir behind a porous wall at $x = -1$ and

Figure 1: The one-dimensional diffusion flame between two porous walls.

that the oxidizer diffuses from the free stream through the porous wall at $x = 1$, see Figure 1. The equations governing the flame evolution over time $t > 0$ can be written as

$$\frac{\partial T}{\partial t} = \frac{\partial^2 T}{\partial x^2} + w - RD(T^4 - T_0^4), \tag{1}$$

$$L\frac{\partial Y_o}{\partial t} = \frac{\partial^2 Y_o}{\partial x^2} - w, \tag{2}$$

$$L\frac{\partial Y_f}{\partial t} = \frac{\partial^2 Y_f}{\partial x^2} - w. \tag{3}$$

Here $T = T(x,t)$ denotes the temperature, Y_o is the oxidizer mass fraction and Y_f gives the fuel mass fraction of the mixture. L is the Lewis number, taken to be the same for fuel and oxidizer, and R is the ratio of characteristic chemical and radiation time scales. In the limit as $R \to 0$ chemistry dominates and radiation becomes unimportant. The nondimensional reaction term w for the one-step reaction is given by

$$w = DY_oY_fe^{-T_a/T} \tag{4}$$

where D is the Damköhler number and T_a is the activation temperature. We assume the following boundary conditions at the porous walls:

$$\text{at } x = -1: \quad T = T_0,\ Y_f = 1,\ Y_o = 0, \tag{5}$$

$$\text{at } x = +1: \quad T = T_0,\ Y_f = 0,\ Y_o = 1. \tag{6}$$

This model has been studied extensively before. In particular, nondimensionalization was carried out exactly as in Sohn et al. [12]. A slightly different configuration is preferred by Matalon and his coworkers [1, 2]. Christiansen et al.[3] added many complicated real-world influences. For a discussion of radiative loss see T'ien [13]. They all provide excellent physical descriptions of diffusion flames and cite many references.

The equations used by Sohn et al. [12] are equivalent to the above equations (1-6) when $T_a = 5$, $T_0 = 0.1$ and $L = 1$. Except for a brief discussion in the next Section 3, we shall also take $L = 1$. We shall keep $T_0 = 0.1$. In our experience, the introduction of other parameters, like the Peclet number of convection, different starting fuel fractions Y_f at $x = -1$ and different wall temperatures T_0 do not change the resulting stability behavior substantially.

Our analysis starts with finding steady state solutions of (1-6). When radiation is neglected ($R = 0$) plotting $T(x = 0)$ of the steady solution vs. D gives the classical S-curve, see Figure 2. We will show that as R increases the S-curve typically breaks into 2 pieces: an island (isola) and an ignition branch (This does not happen at low T_a). We investigate the stability of each steady state by examining eigenvalues of the system linearized around the steady state solution. In particular, let $\bar{T}, \bar{Y}_o, \bar{Y}_f$ be a steady solution. Using

$$T(x,t) = \bar{T}(x) + e^{\sigma t}u(x) \tag{7}$$

$$Y_o(x,t) = \bar{Y}_o(x) + e^{\sigma t}y_o(x) \tag{8}$$

$$Y_f(x,t) = \bar{Y}_f(x) + e^{\sigma t}y_f(x) \tag{9}$$

in (1-6) and neglecting nonlinear terms leads to the following eigenvalue problem

$$\sigma u = u'' + \omega - 4RD\bar{T}^3u \tag{10}$$

$$L\sigma y_o = y_o'' - \omega \tag{11}$$

$$L\sigma y_f = y_f'' - \omega \tag{12}$$

$$u = y_o = y_f = 0 \quad \text{at} \quad x = \pm 1, \tag{13}$$

where

$$\omega = D(\bar{Y}_oy_f + y_o\bar{Y}_f + \bar{Y}_o\bar{Y}_fT_au/\bar{T}^2)e^{-T_a/\bar{T}}. \tag{14}$$

The difference between equations (11) and (12) gives $L\sigma(y_o - y_f) = (y_o - y_f)''$. Hence, when $y_o \neq y_f$ the boundary condition (13) implies that $L\sigma = -(n\pi/2)^2$ for some $n \geq 1$. This gives one branch of eigenvalues.

It is easy to see [9] that the system (10-14) has a nontrivial solution for infinitely many eigenvalues σ, which have no finite accumulation point. It is well known [4, 9] that if all eigenvalues σ have negative real parts then all solutions of (1-6) that start as small perturbations of the steady state solution decay exponentially to the steady state, i.e. the steady state is stable. The steady state is unstable [4, 9] if there exists an eigenvalue σ with a positive real part, in which case there exists a number $r > 0$ such that for every number $\epsilon > 0$ one can find a perturbation of the steady solution which is initially closer to the steady solution than ϵ yet eventually differs from it by more than r.

On the graphs we will use thick curves to denote stable steady states and thin curves to denote unstable states. When the leading eigenvalue is complex the curve will be dashed. For example, in Figure 2, the leading eigenvalue is positive between the lower turn and the point labeled 4, it is complex with positive real part between 4 and 5, it is complex with negative real part between 5 and 6 and it is negative after 6.

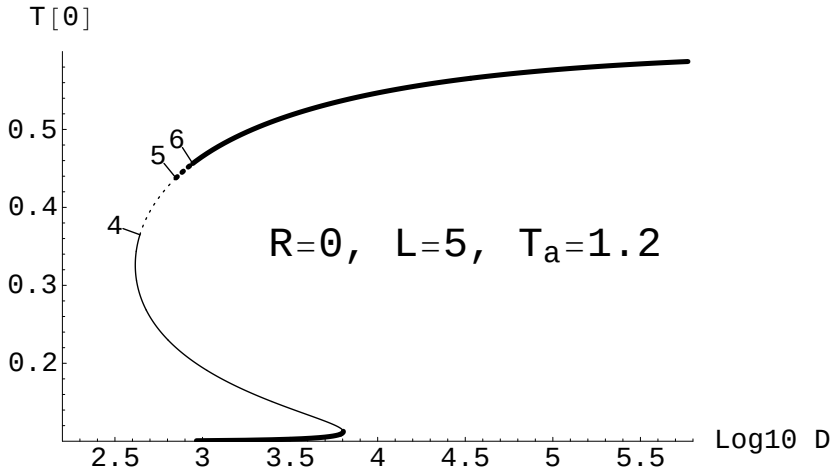

Figure 2: S-curve of steady states and their stability.

Every unstable state could be stabilized if oscillations in a second space direction would be allowed. To see that when $L = 1$, replace $\partial/\partial x^2$ with Δ and introduce spatial oscillations in a direction orthogonal to x, with a wave number k. This leads to a simple shift of eigenvalues, $\sigma \to \sigma - k^2$. This was observed in [1, 14] and leads to many interesting cellular flames. When $L \neq 1$ a similar shift occurs but there is no such simple formula for the shift - see the Appendix for the proof of stabilization for large k at any $L > 0$.

A Hopf bifurcation [4] occurs when the leading eigenvalue is complex and its real part changes sign. On Figure 2 this happens at point 5. It is either supercritical or subcritical. When it is supercritical a stable time periodic solution (= SPO = stable limit cycle) of (1-6) exists near the bifurcation point on the side where the leading eigenvalue has a positive real part. In other words, small perturbations of unstable steady states near the supercritical bifurcation evolve into a stable time periodic solution of (1-6). As an example, in Figure 3 we have supercritical Hopf bifurcations at points marked by SPO

- perturbations of the unstable steady flames between them result in a stable oscillatory flame (see Figure 6). When the bifurcation is subcritical an unstable periodic solution

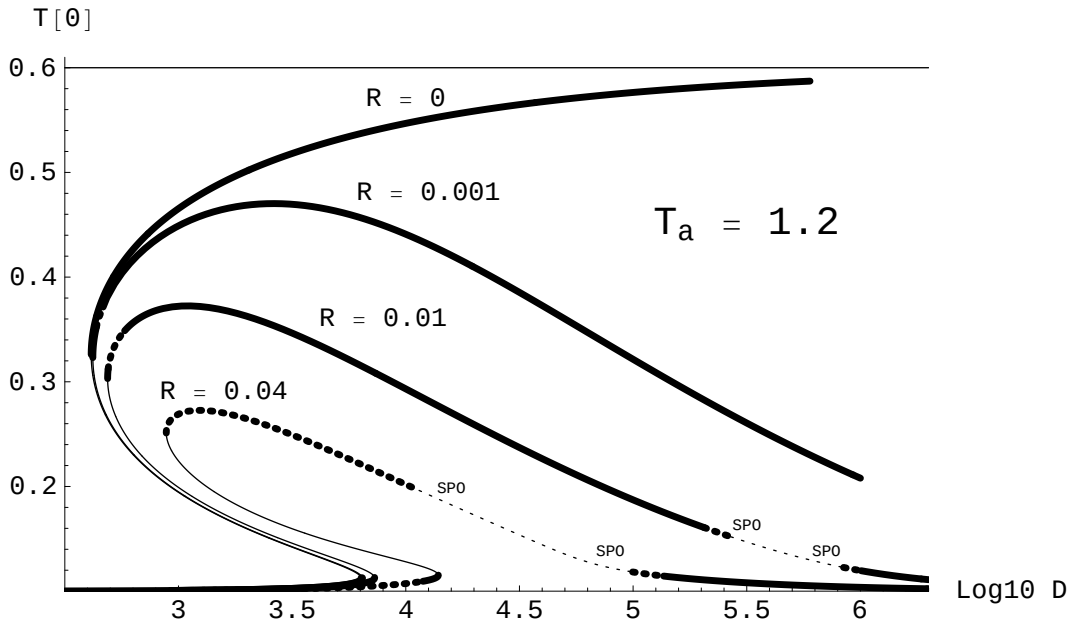

Figure 3: Changes in the S-curve as radiation R increases. We have stable periodic oscillations (SPO) at the points indicated, due to the appearance of a supercritical Hopf bifurcation.

exists on the side where the leading eigenvalue has a negative real part. Small perturbations of unstable steady states near the subcritical bifurcation point lead to extinction, as illustrated in Figure 5. We have a subcritical bifurcation at point 5 on Figure 2.

We find steady states by using the shooting method with Newton's method for finding zeros. This can be done fast if a suitable continuation method is employed. We use either continuation in D or in $T'(-1)$ and we must switch several times when islands appear. For each steady state we solve a higher order discretized version of the eigenvalue problem (10-14). This information is presented by graphs like Figure 2. To determine the type of Hopf bifurcation we make a small initial perturbation of an unstable steady state solution near the bifurcation point and solve (1-6) directly using a higher order finite difference scheme. It is important to be close enough to the bifurcation point and for the size of the perturbation to be small enough; the perturbation shape does not matter. However, if one is too close to the bifurcation point or the perturbation is too small, then it takes too long to determine whether a periodic solution evolves, see Figure 4. A careful analysis of small oscillations actually provides a very good independent verification of the steady solution and of the leading eigenvalue since it determines the growth rate and frequency of the oscillations.

3 Hopf bifurcations when $R = 0$.

Much previous work has been done in this case [3, 8, 11, 12, 14]. Steady state solutions form the S-curve shown in Figure 2. There exists an $L_{crit} > 1$ such that if $L < L_{crit}$ then the upper branch consists of stable steady state solutions and the middle branch consists of unstable steady state solutions. When $L > L_{crit}$ the stability picture looks like the one in Figure 2 with the Hopf bifurcation at point 5. We made many calculations for many different values of the physical parameters, yet we always found the bifurcation to be subcritical when $R = 0$.

The growth or the decay of small perturbations, as obtained directly from (1-6), is very slow if the steady state is very close to the bifurcation point. For example, Figure 4 shows

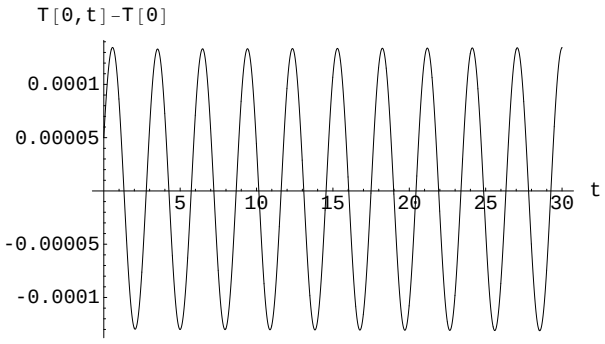

Figure 4: $R = 0$, $L = 5$, $T_a = 1.2$, $\bar{T}(0) = 0.44$. Unstable oscillations at $D = 703.5$ (bifurcation at $D = 703.64$) that lead to extinction, as on Figure 5, after about 5300 periods. The growth is exponential but at first is very slow and virtually unnoticable.

only about a 1% growth in amplitude after the first cycle. A first noticable increase in the growth rate in this case happens if we start with a 300 times larger initial perturbation (or continue for about 5000 periods), and it leads to extinction after about an 800 times larger initial perturbation, see Figure 5. This contrasts sharply with statements made by Sohn et

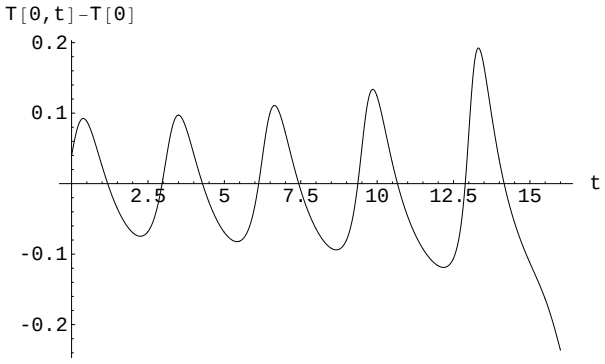

Figure 5: As on Figure 4 but with 800 times larger initial perturbation.

al. in [12] and in the previous nonlinear analysis (Sohn et al. in [11]), concluding that the oscillations should be terminated after a few cycles. However, it is unlikely that an actual

experiment would produce these kind of oscillations which would last virtually unchanged for hundreds of cycles. The key reasons for being able to produce graphs like Figure 4 is the ability to choose D very close to the bifurcation value and make small perturbations of the unstable steady state. For example, if the Damköhler number is dropped to $D = 700$ from $D = 703.5$ the growth rate jumps from 0.0004 to .0100, i.e. a 0.5% drop in the Damköhler number causes a 25 fold increase in growth rate, which shortens the period of persistence of oscillations by roughly a factor of 25.

The frequency of these types of oscillations decreases to 0 as $L \to L_{crit}$ - hence they allow for arbitrarily long periods. They have been studied extensively by Christiansen et al. [3]. Nayagam and Williams [10] observed them in experiment.

The same observations apply whenever the bifurcation is subcritical, even when radiation is accounted for. However, we will focus on supercritical bifurcations from now on. At fixed R we may have both supercritical and subcritical bifurcations. For example, when $R = 0.2$ in Figure 14 we have a subcritical bifurcation at the top and two supercritical bifurcations on the back of the curve (and this is not limited to low T_a).

4 Islands and oscillations when $R > 0$ and $T_a = 1.2$.

We use $L = 1$ in the rest of the article.

We shall now describe the appearance and disappearance of islands (isolas) as well as the appearance of a supercritical Hopf bifurcation when we account for radiation. We chose a very low activation temperature $T_a = 1.2$ to start the discussion because at this T_a it is much easier to show the evolution of the stability diagram. We found essentially exactly the same behavior for all $T_a > 1$ that we analyzed - we will later show some results also for $T_a = 3$ to highlight changes with increasing activation temperature.

Let us focus on Figure 3 first. Note that if $R = 0$ then $T(0) \to 0.6$ as $D \to \infty$ which is the Burke-Schumann limit. On the other hand, when radiation is accounted for $T(0) \to 0$ as $D \to \infty$. This asymptotic behavior is discussed in more detail in Section 6.

When $R = 0.01$, supercritical Hopf bifurcations occur at $D = 268973$ and $D = 843180$ on the back of the S-curve, see Figure 3. Between the bifurcation points the steady states are linearly unstable, however, perturbations of all those unstable states lead to stable oscillations as shown in Figure 6. Now, let us look at the leading eigenvalue, which is

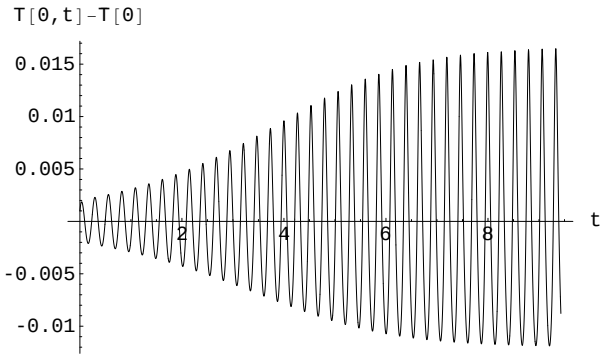

Figure 6: Evolution of stable oscillations near $D = 797500$, $R = 0.01$, $T_a = 1.2$. Although the steady state is unstable, the perturbations of it lead to stable oscillations.

complex and has a positive real part between the two bifurcation points. As D decreases the real part of the leading eigenvalue quickly sinks under the constant eigenvalue $-(\pi/2)^2$, however, it re-emerges as a leading eigenvalue near the upper turn. As D further decreases the eigenvalue splits into two real eigenvalues, the largest of them becomes 0 at the turn and becomes positive on the middle branch. The difference between (11) and (12) is responsible for the eigenvalue $-(\pi/2)^2$.

As R decreases the region where the leading eigenvalue is complex and has positive real part shrinks and disappears at $R = 0.0063$, $D = 1.0 \times 10^6$. Hence, when $R < 0.0063$ the whole upper branch is stable, see Figure 3.

As R increases to $R = 0.04$, Figures 3 and 7, the real part of the leading eigenvalue increases, at the turn we still have the same behavior of the eigenvalue as when $R = 0.01$ and between the bifurcation points we have stable oscillations which will be discussed below.

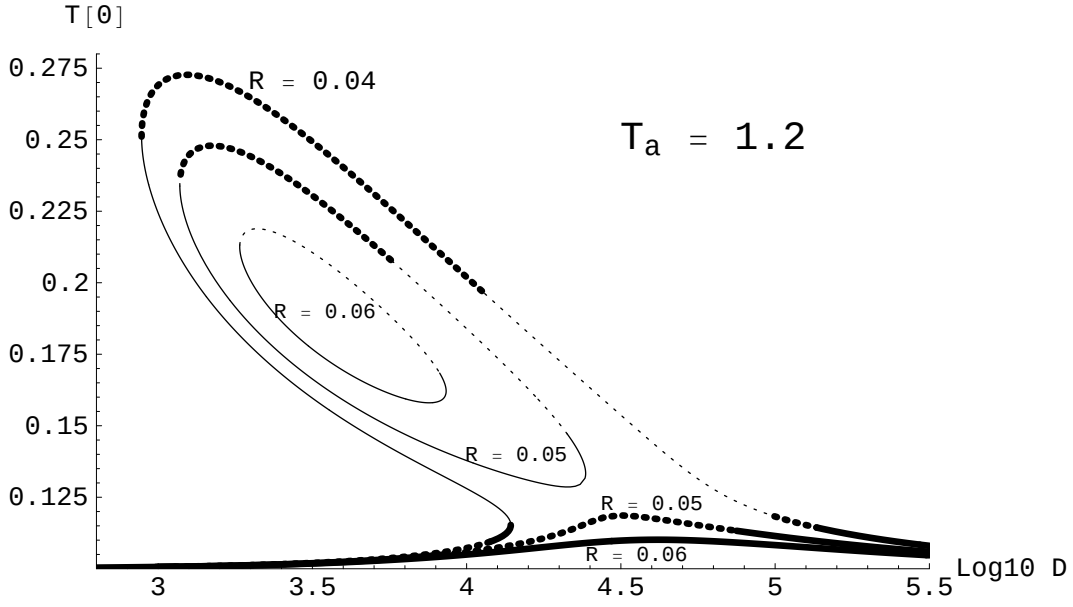

Figure 7: The island is formed from the S-curve near $R = 0.05$ and it disappears for $R > 0.07$ - the lower ignition branch remains.

The top part of the S-curve gets pinched off near $R = 0.05$ creating an island and a lower branch, see Figure 7. As R increases further, the island shrinks and disappears near $R = 0.07$. The lower branch persists and approaches closer and closer to $T_0 = 0.1$. We were not able to find stable oscillations near the bifurcation point on the island at $R = 0.05$. At higher values of T_a we do find stable oscillations near the bifurcation point on the island when R is close to the value at which the island is created. Note that all the steady states on the island are unstable when $R = 0.06$ - hence there is no Hopf bifurcation point on the island.

Now, let us have a closer look at the stable oscillations. Figure 6 shows a slight amount of asymmetry between times spent at high vs. low temperature, which becomes more pronounced further away from the bifurcation point. The asymmetry increases

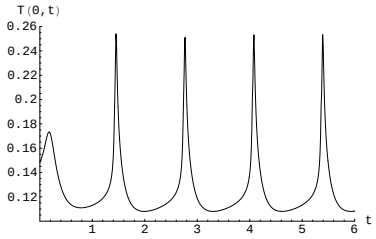

Figure 8: Evolution of stable oscillations at $D = 40000$, $R = 0.04$. $\bar{T}(0) = 0.1441$.

considerably at $R = 0.04$, see Figure 8. When $R = 0.04$ bifurcations occur at $D = 11368$

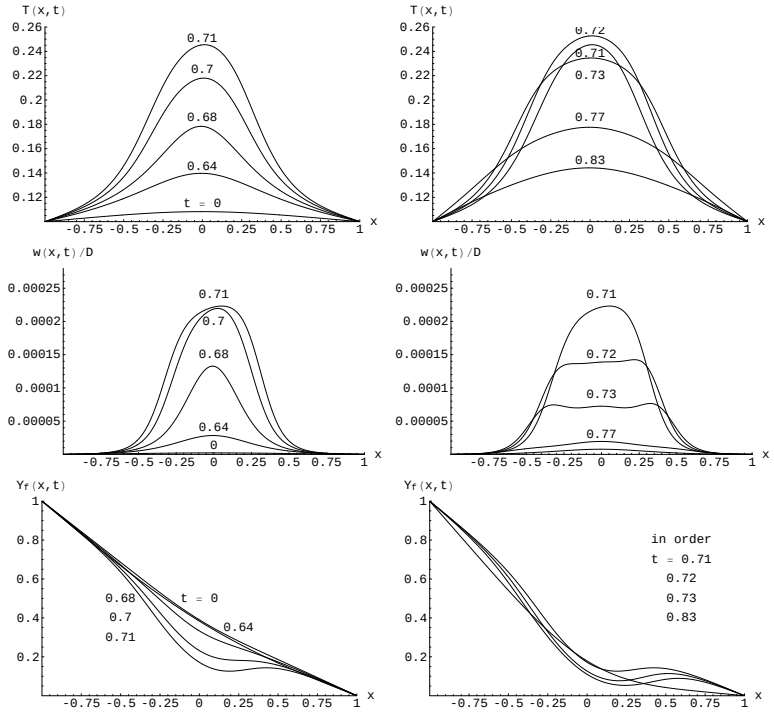

Figure 9: Detailed examination of one cycle on Figure 8. The cycle length is 1.313.

and $D = 99561$ and between them all unstable states evolve into stable periodic solutions. The growth rate of linear oscillations is the largest near $D = 40000$, hence the transition is very fast on Figure 8. Note that the flame temperature is for the most part of the cycle close to the surrounding temperature $T_0 = 0.1$, however, it bursts, for a short time, beyond the unstable steady state temperature close to the highest stable steady temperature at $R = 0.04$, see Figure 7. Details on Figure 9 seem to suggest that the burst causes fuel depletion, hence the dip in Y_f, which takes a long time to recover.

5 Islands and oscillations when $R > 0$ and $T_a = 3$.

When $T_a = 3$ the islands are created near $R = 3.1 \times 10^{-9}$ the same way as when $T_a = 1.2$, see Figures 10, 11, 12 below.

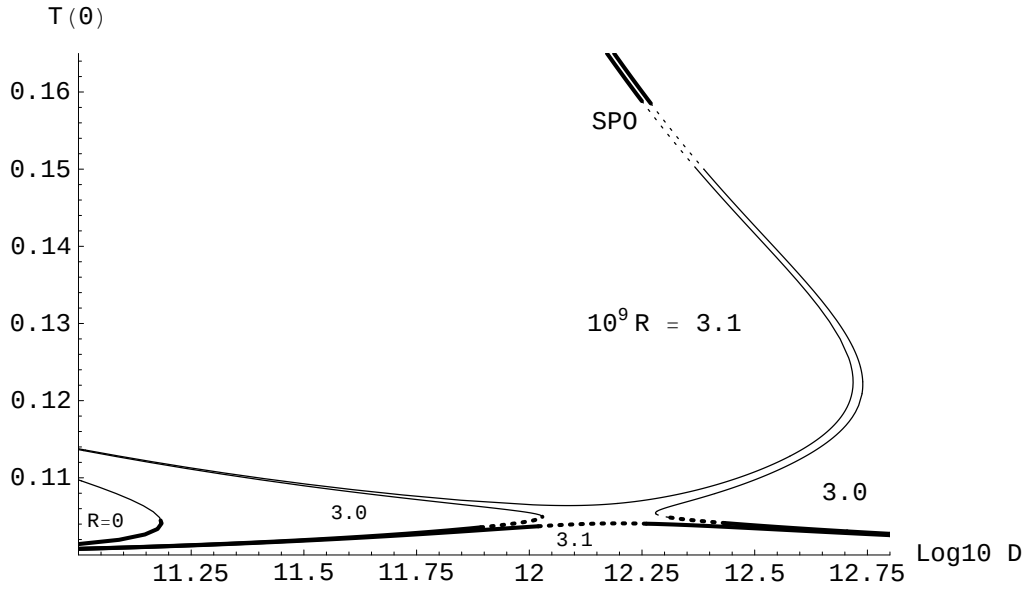

Figure 10: Creation of an island at $T_a = 3$. At SPO a supercritical Hopf bifurcation occurs.

In Figure 10, near SPO, the real part of the leading eigenvalue increases with D very fast, so, as D decreases it dips under the constant eigenvalue $-(\pi/2)^2$ too fast to be shown in the figure, hence a regular Hopf bifurcation occurs at SPO even though the picture can not show it. We found that stable oscillations with period of about 0.04 evolve from perturbations of unstable steady states near SPO. As R decreases the region with unstable states on the back shrinks and then disappears as in Figures 3 and 14.

We take a closer look at Figure 12 when $R = 10^{-5}$. Between 1 and 2 the leading eigenvalue is complex with a positive real part. At 2 the real part changes sign and it sinks under the constant eigenvaule at 3. The leading eigenvalue between 3 and 4 has the value $-(\pi/2)^2$. At 4 the complex conjugate pair re-emerges as the leading eigenvalue and at 5 it splits into 2 real eigenvalues. The largest of them changes sign at 6. Between 1 and 2, but only near 2, we found stable oscillations. Hence, at 2 we have a supercritical Hopf bifurcation.

When $R = 1.5 \times 10^{-5}$ the same description applies as when $R = 10^{-5}$. When $D = 8 \times 10^6$ we found the period of stable oscillations to be 0.506. There is some asymmetry in the oscillations, but not as pronounced as in Figure 8. The mean temperature of the oscillations is much higher in this case since $\bar{T}(0) = 0.291$.

When $R \geq 2 \times 10^{-5}$ we were no longer able to find stable oscillations on the island. As Figure 12 shows, the island still has stable steady solutions when $R = 5 \times 10^{-5}$, but their number decreases as R increases. All steady states on the island are unstable at $R = 6.4 \times 10^{-5}$; the island disappears near $R = 7 \times 10^{-5}$ even though the lower branch that is very close to $T_0 = 0.1$ remains.

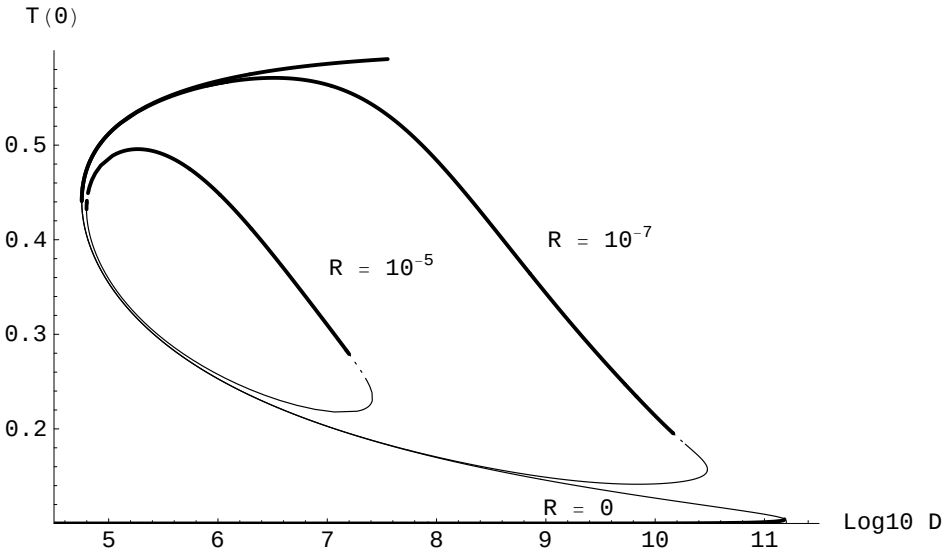

Figure 11: Islands and S-curve when $T_a = 3$.

6 Reaction sheet limit

We examinined the behavior of solutions on the back (large D) of the islands and the back of S-curves for large D. The reactivity w, equation (4), resembles a delta function, the fuel fraction of the mixture decreases linearly to 0 at $x = 0$ and there is almost no fuel in the region $x > 0$. For the oxidizer the reverse is true. Using $w = \delta(x)$ in the time independent version of (1-3) implies that $\bar{Y}_o'$, $\bar{Y}_f'$ and $-\bar{T}'$ jump by 1 at $x = 0$. This and the symmetry of $\bar{T}$ imply

$$\bar{Y}_f(x) = -x, \quad \bar{Y}_o(x) = 0 \quad \text{for } -1 \le x < 0, \tag{15}$$

$$\bar{Y}_f(x) = 0, \quad \bar{Y}_o(x) = x \quad \text{for } 0 < x \le 1, \tag{16}$$

$$\bar{T}''(x) = RD(\bar{T}(x)^4 - T_0^4) \quad \text{for } 0 \le x \le 1, \qquad \bar{T}'(0) = -1/2,\ \bar{T}(1) = T_0. \tag{17}$$

In other words, we have a reaction sheet at $x = 0$ in the Burke-Schumann limit of infinitesimally thin reaction zone with added radiative heat loss. Equation 17 implies that $\bar{T}(0)$ is given by

$$\int_{T_0}^{\bar{T}(0)} \frac{2\,dT}{\sqrt{1 + 8RD((T^5 - \bar{T}(0)^5)/5 - T_0^4(T - \bar{T}(0)))}} = 1. \tag{18}$$

We note that the solution depends only on the composite parameter RD in this infinite-rate chemistry limit. We solved (18) for $\bar{T}(0)$ and plotted it vs. D in Figure 13. Note that when $RD = 0$ we recover the non-radiative Burke-Schumann limit $\bar{T}(0) = 1/2 + T_0 = 0.6$, and for small RD we obtain

$$\bar{T}(0) \doteq 1/2 + T_0 - RD(320T_0^3 + 180T_0^2 + 48T_0 + 5)/480 \qquad \text{for small } RD. \tag{19}$$

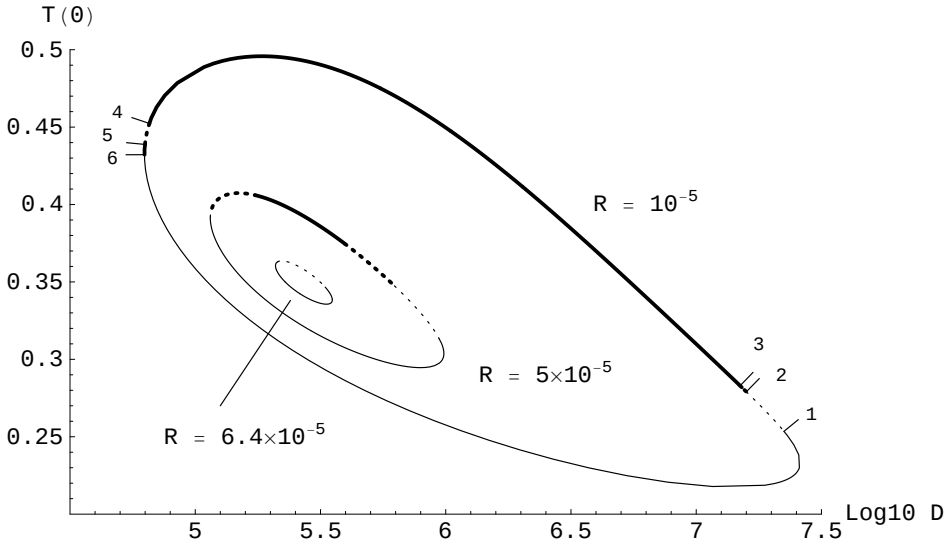

Figure 12: Details on the islands when $T_a = 3$.

Note also that as R decreases the steady state solutions on the back of S-curves approach very close to their reaction sheet limit.

In order to keep the dominator in (18) positive for large RD we need $\bar{T}(0) - T_0$ to be small. Setting the dominator to zero at $T = T_0$ and inverting the series up to quadratic terms in $(\bar{T}(0) - T_0)/T_0$ gives

$$\bar{T}(0) \doteq T_0 + \frac{4T_0}{1 + 8\sqrt{RDT_0^5} + \sqrt{64RDT_0^5 + 16\sqrt{RDT_0^5} - 1}} \qquad \text{for large } RD. \tag{20}$$

It turns out that (20) produces an error smaller than 10^{-5} when $RD > 10^4$ (recall, $T_0 = 0.1$). One can show that the correction to (20) which would account also for the equality in (18) is actually exponentially small.

7 Conclusions

We shall organize our conclusions in order of increasing R at any given T_a. "Small R" ... has quite a different range of values at different values of T_a.

When R is very small the back of the S-curve gets pushed down to T_0 and the whole upper branch is stable as seen in Figure 13. The back of the S-curve is very close to the reaction sheet limit when R is very small (Figure 13).

As R increases an interval of unstable steady states appears on the back of the S-curve. When these steady states are slightly perturbed they evolve into stable oscillations because supercritical Hopf bifurcations occur at the two ends of the region. A typical example can be seen in Figure 3 ($R = 0.01$). For smaller values of T_a perturbations of all unstable states in the interval lead to stable oscillations. For larger values of T_a only states near the bifurcation points evolve into stable oscillations.

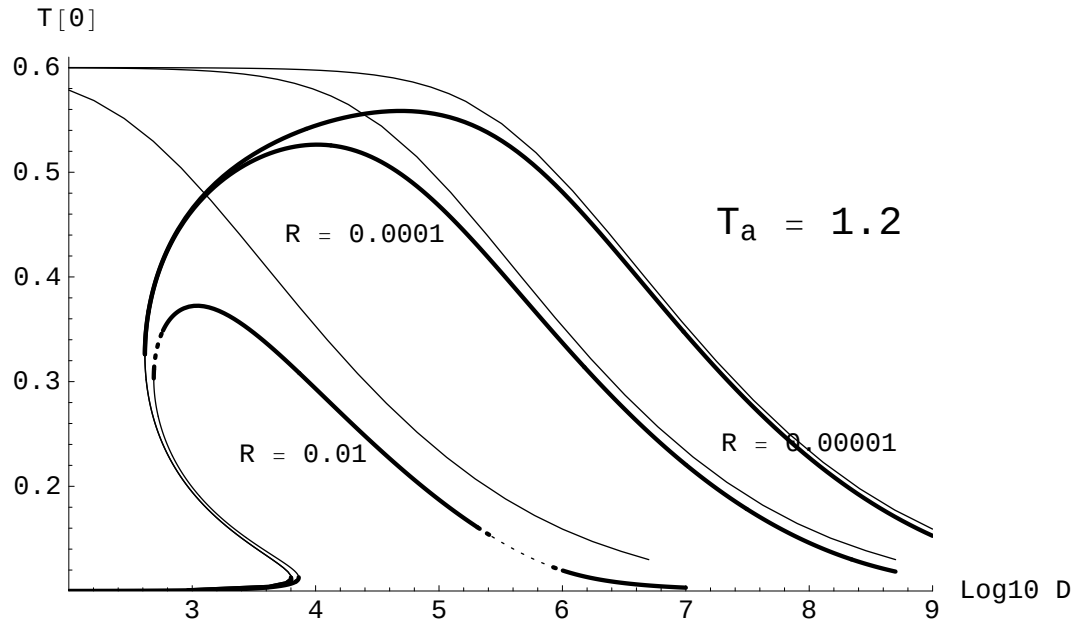

Figure 13: S-curves with the corresponding reaction sheet limits from equation (18)

When $T_a = 1$ the S-curve simply flattens out as R increases further, see Figure 14.

When $T_a > 1$ the S-curve breaks at a certain value of R, creating an island (isola) and a lower branch (Figures 7, 10). As R further increases the island becomes a collection of completely unstable steady states that eventually disappears. The lower branch persists.

T_a	R_{appear}	$R_{disappear}$
1.1	0.1111	0.117
1.2	.05	0.07
2	3.9×10^{-5}	1.9×10^{-3}
3	3.1×10^{-9}	7×10^{-5}
5	1.2×10^{-17}	3.1×10^{-7}
6	6.7×10^{-22}	2.9×10^{-8}

Table 1: T_a vs. values of R where the islands appear and disappear.

Right after the island appears we have a Hopf bifurcation on the back of the island, as shown in Figure 10. At high values of T_a the bifurcation is supercritical - implying the appearance of stable oscillations. This was first observed by Sohn et al. [12]. At smaller values of T_a we determined that the bifucation is actually subcritcal - implying no stable oscillations on any island (Figure 7). We found that as R increases the Hopf bifurcation always becomes first subcritical and then it disappears.

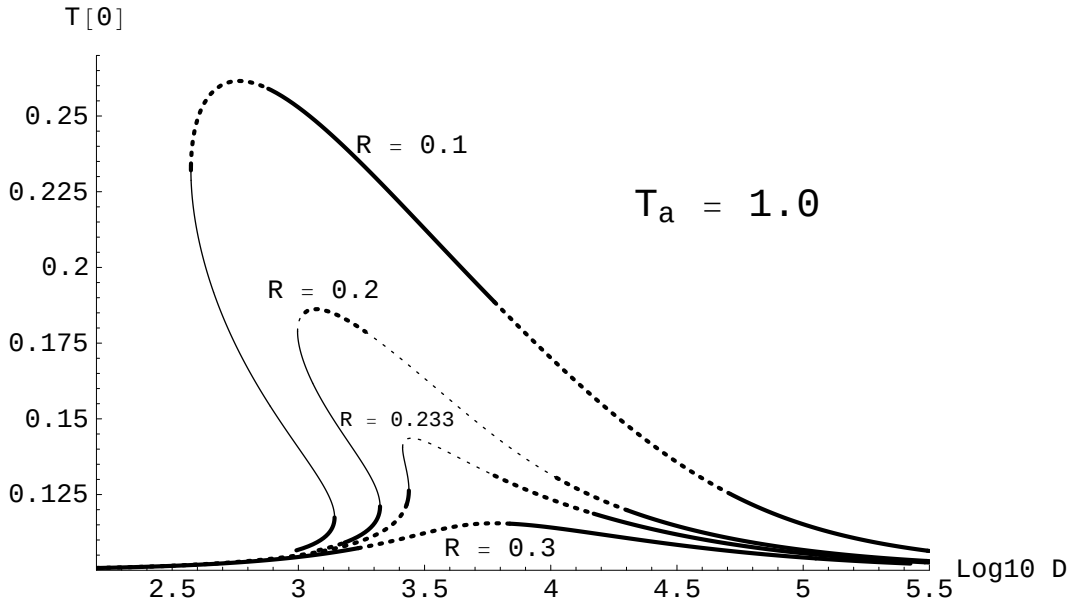

Figure 14: No islands appear when $T_a = 1$. The region of unstable steady states was first observed near $R = 0.1113$ and $D = 20000$. All unstable steady states on the backs of the curves evolve into stable oscillations.

8 Appendix

Here we want to show that every steady state solution can be stabilized if spatial ocillations in a direction orthogonal to x-direction are allowed. Equations (10, 11,12) modified to account for the oscillations with a wave number k are

$$\sigma u = u'' - k^2 u + \omega - 4RD\bar{T}^3 u$$

$$L\sigma y_o = y_o'' - k^2 y_o - \omega$$

$$L\sigma y_f = y_f'' - k^2 y_f - \omega.$$

Multiplying these equations with $\bar{u}, \bar{y}_o, \bar{y}_f$, integrating from -1 to 1 and using boundary conditions (13) gives

$$\sigma \int |u|^2 = -\int |u'|^2 - k^2 \int |u|^2 + \int \omega\bar{u} - 4RD \int \bar{T}^3 |u|^2$$

$$L\sigma \int |y_o|^2 = -\int |y_o'|^2 - k^2 \int |y_o|^2 - \int \omega\bar{y}_o$$

$$L\sigma \int |y_f|^2 = -\int |y_f'|^2 - k^2 \int |y_f|^2 - \int \omega\bar{y}_f.$$

Define

$$h = \sqrt{|u|^2 + |y_o|^2 + |y_f|^2}$$

hence

$$\mathrm{Re}(\sigma)\int h^2 \le -k^2\min\{1,1/L\}\int h^2 + \mathrm{Re}\int \omega(\bar{u}-\bar{y}_o/L-\bar{y}_f/L) - 4RD\int \bar{T}^3|u|^2.$$

Using Schwarz inequality in equation (14) gives a real number C such that

$$\mathrm{Re}\,\omega(\bar{u}-\bar{y}_o/L-\bar{y}_f/L) - 4RD\bar{T}^3|u|^2 \le Ch^2.$$

Therefore

$$\mathrm{Re}(\sigma) \le C - k^2\min\{1,1/L\}$$

hence at any fixed $L>0$ one can find k such that all eigenvalues become negative.

References

[1] Cheatham S and Matalon M, Heat Loss and Lewis Number Effects on the Onset of Oscillations in Diffusion Flames, *Proceedings of the 26th Symposium on Combustion*, 26 (1996), 1063-1070

[2] Cheatham S and Matalon M, A General Asymptotic Theory of Diffusion Flame with Application to Cellular Instability, *J. Fluid Mech.*, 414(2000), 105-144

[3] Christiansen E W, Tse S D and Law C K, A Computational Study of Oscillatory Extinction of Spherical Diffusion Flames, *Combustion and Flame*, 134(2003), 327-337

[4] Henry D 1981 *Geometric Theory of Semilinear Parabolic Equations (Lecture Notes in Mathematics, vol. 840)* (Berlin: Springer)

[5] Kim J S, Linear Analysis of Diffusional-Thermal Instability in Diffusion Flames with Lewis Numbers Close to Unity, *Comb. Th. Model.*, 1(1997), 13

[6] Kim J S, Lee S R, Diffusional-Thermal Instability in Strained Diffusion Flames with Unequal Lewis Numbers, *Comb. Th. Model.*, 3(1999), 123

[7] Kim J S, Williams F A, Ronney P D, *J. Fluid Mechanics*, 327 (1996) 273-301

[8] Kukuck S, Matalon M, The onset of oscillations in diffusion flames, *Combust. Theory Modelling*, 5 (2001) 217-240

[9] Miklavčič M 1998 *Applied Functional Analysis and Partial Differential Equations* (Singapore: World Scientific)

[10] Nayagam V, Williams F A Dynamics of diffusion flame oscillations prior to extinction during low gravity droplet combustion, *7th Int. Conf. on Numerical Combustion* 1998 (New York: SIAM)

[11] Sohn C H, Chung S H, Kim J S, Instability-Induced Extinction of Diffusion Flames Established in the Stagnant Mixing Layer, *Combust. Flame*, 117(1999) 404-412

[12] Sohn C H, Kim J S, Chung S H, Maruta K, Nonlinear Evolution of Diffusion Flame Oscillations Triggered by Radiative Heat Loss, *Combust. Flame*, 123(2000) 95-106

[13] T'IEN J S, Diffusion Flame Extinction at Small Stretch Rates: The Mechanism of Radiative Loss, *Combustion and Flame*, 65(1986), 31-34

[14] VANCE R, MIKLAVČIČ M, WICHMAN I S, On stability of one dimensional diffusion flames, *Combust. Theory Modelling*, 5 (2001) 147-161